Hybrid Electrolyzer Configuration for Efficient CO_2 Electrolysis

Ismail, Ahmed Mohsen; Lawrence, Katherine R.; Kortlever, Ruud

DOI
10.1021/acsenergylett.5c02368

Publication date
2025

Document Version
Final published version

Published in
ACS Energy Letters

ACS Energy LETTERS

http://pubs.acs.org/journal/aelccp

ENERGY EXPRESS

Hybrid Electrolyzer Configuration for Efficient CO_2 Electrolysis

Ahmed Mohsen Ismail, Katherine R. Lawrence, and Ruud Kortlever*

Cite This: *ACS Energy Lett.* 2025, 10, 5228−5231

Read Online

ACCESS | Metrics & More | Article Recommendations | Supporting Information

ABSTRACT: **We demonstrate a hybrid electrolyzer design for CO_2 electrolysis to multicarbon products using a cation exchange membrane and different electrode separations. Reducing the thickness of the catholyte flow field from 5 to 2.4 mm significantly decreases the cell voltage while maintaining longer-term stability.**

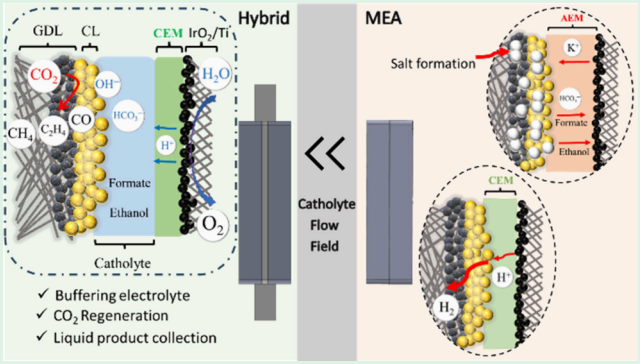

In recent years different electrolyzer architectures have been employed for CO_2 electrolysis.[1−3] Membrane electrode assembly (MEA) electrolyzers with an anion exchange membrane (AEM) are widely used to suppress the competing hydrogen evolution reaction (HER). However, AEMs allow the crossover of (bi)carbonate and anionic products.[4,5] This crossover is detrimental to CO_2 electrolyzers as it complicates downstream separation processes and lowers the CO_2 utilization due to (bi)carbonate transport to the anolyte with subsequent CO_2 release at the anode.[6,7] In addition to poor anion selectivity, AEMs can allow cations (such as K^+) to migrate to the cathode, particularly at high current densities. These cations form salts with (bi)carbonate ions, which negatively affect the long-term durability of the gas diffusion electrodes (GDEs).[8,9] Furthermore, collecting liquid product in MEA electrolyzers is challenging due to the absence of a catholyte and the potential crossover of generated products through the AEM. Remarkably, over 80% of the liquid products generated at the cathode of a MEA electrolyzer have been reported to cross the AEM to the anode.[10] Additionally, the literature lacks a discussion on the potential impact of vapor phase liquid product diffusion back through the GDE on the stability of the catalyst layer and the hydrophobicity of the gas diffusion layer (GDL).

To address the challenges associated with the crossover and collection of the liquid product in MEA electrolyzers, cation exchange membranes (CEM) and bipolar membranes (BPM) have been proposed as effective solutions to prevent crossover issues. However, with these membranes in a MEA configuration, the local chemical environment becomes acidic, which facilitates the kinetics of HER over electrochemical CO_2 reduction (CO_2R).[5,7] Several strategies have been developed to better control the local environment for selective CO_2R. One approach involves coating the cathode GDE with a thin anion exchange polymer (<10 μm thick) to create a CO_2 regeneration layer. Using this coating process, a single-pass CO_2 conversion of 85% at 100 mA/cm^2, along with a faradaic efficiency (FE) for multicarbon products of 55% at 125 mA/cm^2 was achieved.[7] Another strategy involves designing a three-compartment hybrid cell. A porous solid ion conductor was placed in the middle compartment between the AEM and CEM membranes to facilitate efficient ion transfer. This configuration achieved the generation of 2 M formic acid at a current density of 200 mA/cm^2 with a FE of 80.1%, using 100 mL/min of humidified N_2 gas passing through the middle compartment.[11] However, scaling up the MEA hybrid cell remains challenging due to presence of the solid electrolyte between the AEM and CEM. Therefore, most MEA hybrid systems are limited to an active surface area smaller than 10 cm^2.[2] An alternative hybrid configuration features a liquid catholyte layer between the cathode and the membrane while maintaining a zero-gap arrangement between the anode and the membrane.[12] This was demonstrated earlier in a hybrid cell

Received: July 28, 2025
Revised: September 25, 2025
Accepted: September 26, 2025

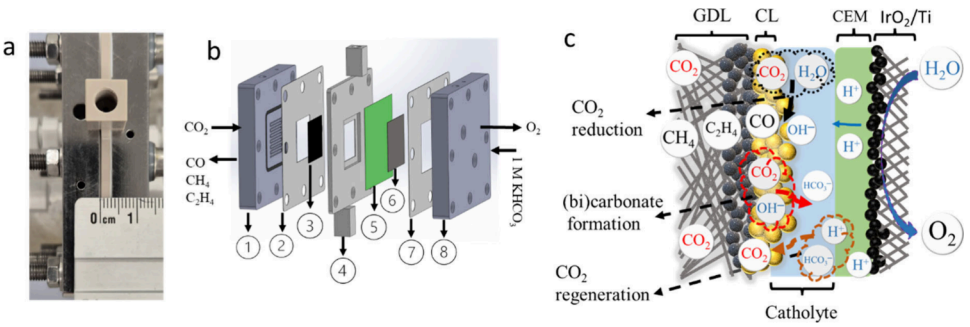

Figure 1. Overview of the hybrid CO_2 electrolyzer design. (a) A photograph showing a top view of the assembled hybrid electrolyzer cell with a 2.4 mm thick catholyte flow field between the cathode gas diffusion electrode and the membrane, sealed by two 0.3 mm gaskets, resulting in a 3 mm electrode separation. (b) A detailed illustration showcasing the components of a hybrid electrolyzer cell: (1) cathode current collector, (2) gasket, (3) cathode copper gas diffusion electrode, (4) catholyte flow field, (5) cation exchange membrane, (6) anode electrode IrO_2/Ti, (7) gasket, and (8) anode current collector. (c) A schematic illustration of species transport and reactions within a hybrid electrolyzer with a cation exchange membrane.

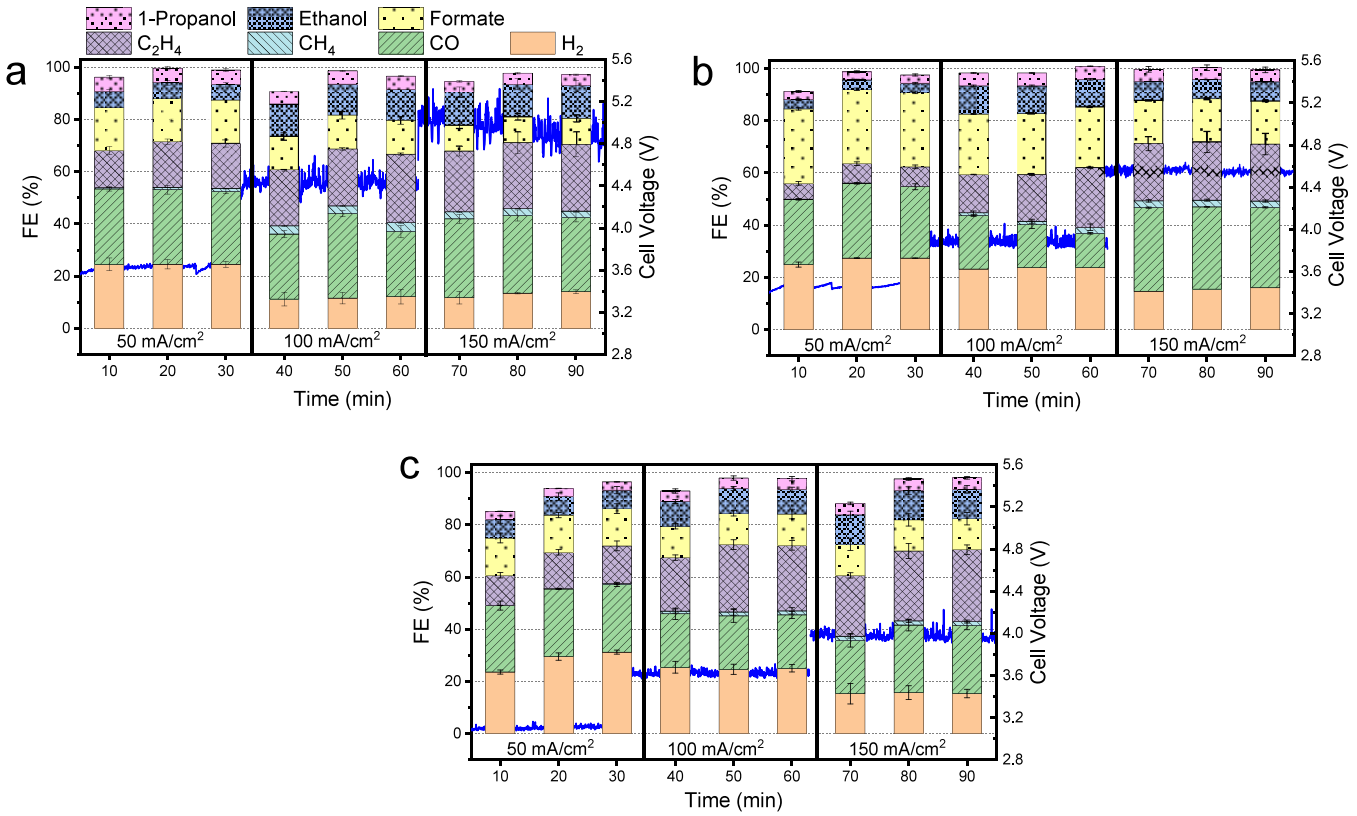

Figure 2. Electrochemical CO_2 reduction performance of Cu GDEs in a hybrid electrolyzer cell with a cation exchange membrane. The Faradaic efficiency of the generated products is plotted as a function of time at current densities of 50, 100, and 150 mA/cm^2 for different catholyte flow field thicknesses (a) 5, (b) 3, and (c) 2.4 mm at a CO_2 flow rate of 20 mL/min. A 1 M $KHCO_3$ solution was used as the catholyte and anolyte. Figure S14 in the Supporting Information displays the cell voltage date at all current densities when using different catholyte flow field thicknesses.

with a 300 cm^2 active area, a silver GDE, and a 2.5 mm electrode separation. Operating at 200 mA/cm^2 and 60 °C, this cell produced carbon monoxide (CO) with an average FE exceeding 90% over 650 h and yielding a cell voltage of 4 V.[13] This performance highlights the applicability of this cell configuration. In contrast, a previous study on CO_2R to multicarbon products using copper (Cu) GDEs and a hybrid electrolyzer with a 6 mm electrode separation resulted in a cell voltage of ~5.5 V and a poor electrolyzer stability.[10] Therefore, there is a need to further explore this system at various catholyte flow field (CFF) thicknesses to take advantage of both the potential for a favorable local environment and minimization of electrode separation. In this Energy Express, we compare the operation of hybrid electrolyzers converting CO_2 to multicarbon products with different electrode separations to provide a systematic study on the impact of CFF thickness on CO_2R efficiency and product selectivity toward desired multicarbon products.

First, we designed three CFFs with different thicknesses: 2.4, 3, and 5 mm (Figure S4). An exploded view illustrating the individual components is depicted in Figure 1b. The use of a catholyte layer allows for the employment of a CEM and

https://doi.org/10.1021/acsenergylett.5c02368
ACS Energy Lett. 2025, 10, 5228−5231

mitigates the impact of the proton flux on the pH profile between the cathode GDE and the membrane.[14] Protons are captured by (bi)carbonate and consumed in the CO_2 regeneration (Figure 1c). To probe the influence of the CFF thickness and assess the efficiency of the electrolyzer, a protocol of three consecutive 30 min chronopotentiometry measurements at current densities of 50, 100, and 150 mA/cm^2 was applied at four different CO_2 flow rates. We refer the interested reader to Section S2 in the Supporting Information for additional details on the electrolyzer setup used for testing. The flow rate of CO_2 has a greater effect on the FEs of hydrogen (H_2) and CO compared to formate and C_{2+} products (Figures S8−S10). At a current density of 150 mA/cm^2, the reaction favored a higher FE toward CO at lower CO_2 flow rates, reaching a peak at 20 mL/min of CO_2, while H_2 FE showed the opposite trend across different CFF thicknesses. A similar result was observed at current densities of 50 and 100 mA/cm^2. A flow rate of 20 mL/min provided the highest selectivity toward CO and ethylene (C_2H_4). Therefore, we discuss the influence of the CFF thickness on the performance of the hybrid electrolyzer at this CO_2 flow rate.

We compared the electrolyzer performance, focusing on cell voltage and product distribution, for different electrode separations. The thickness of the flow field primarily affected the cell voltage. In particular, reducing the thickness from 5 to 2.4 mm at a current density of 150 mA/cm^2 results in a significant cell voltage drop, from 5 to 3.9 V (Figure 2). As shown in Figure S14, the impact of reducing electrode separation becomes more pronounced at higher current densities, where the difference in cell voltage between the electrolyzers increased. In contrast, differences in electrode separation had a minimal effect on the product selectivity. At a current density of 150 mA/cm^2, the H_2 FEs are 15.4%, 16%, and 14% with increasing electrode separation. These low H_2 FEs highlight the role of the catholyte layer in controlling the local chemical environment, particularly the pH (Table S2). Reducing the CFF thickness is an effective way to lower the electrolyte ohmic losses. Moreover, the production of ethylene and ethanol increased with increasing current density, while the FE for the competing HER decreased (Figure 2).

To assess the long-term stability of the electrolyzer, we first ran a chronopotentiometry test for 120 min at 150 mA/cm^2. The hybrid electrolyzer showed a steady cell voltage as well as continuous production across various electrode separations (Figure S15). The experiment was extended to 25 h in a hybrid electrolyzer with a 2.4 mm thick CFF. C_{2+} products and formate FEs remained constant. In the last hour, a slight increase in H_2 FE and a corresponding decrease in CO FE was observed (Figure S16). This 25 h is an order of magnitude longer and operates at a cell voltage that is 1.6 V lower than results from comparable systems in the literature.[10] These improvements in hybrid electrolyzer performance and product stability were enabled by the combination of a well-designed CFF, a buffering electrolyte, and a CEM along with a robust copper carbon-based GDE.

In conclusion, we demonstrate the potential of a hybrid electrolyzer with a liquid catholyte for CO_2 electrolysis to multicarbon products. We show that the thickness of the flow field primarily affects the cell voltage rather than product selectivity. In this work, a hybrid electrolyzer with a CEM and 2.4 mm thick CFF exhibits a stable cell voltage of 3.9 V at a current density of 150 mA/cm^2 without experiencing salt precipitation or product crossover.

■ ASSOCIATED CONTENT

Supporting Information

The Supporting Information is available free of charge at https://pubs.acs.org/doi/10.1021/acsenergylett.5c02368.

Experimental information, including electrode preparation, hybrid electrolyzer configuration, schematic piping, and instrumentation diagram of the test framework; XRD spectra; SEM images; EDS mapping; Electrochemical measurements; ^{1}H NMR spectra; Electrolyte pH and conductivity; Figures S1−S16 (PDF)

■ AUTHOR INFORMATION

Corresponding Author

Ruud Kortlever − *Large-Scale Energy Storage Section, Department of Process and Energy, Faculty of Mechanical Engineering, Delft University of Technology, 2628 CB Delft, The Netherlands; e-Refinery Institute, Delft University of Technology, 2628 CB Delft, The Netherlands;* orcid.org/0000-0001-9412-7480; Email: r.kortlever@tudelft.nl

Authors

Ahmed Mohsen Ismail − *Large-Scale Energy Storage Section, Department of Process and Energy, Faculty of Mechanical Engineering, Delft University of Technology, 2628 CB Delft, The Netherlands; Department of Chemistry, Faculty of Science, Alexandria University, 21511 Alexandria, Egypt; e-Refinery Institute, Delft University of Technology, 2628 CB Delft, The Netherlands;* orcid.org/0000-0002-6899-3577

Katherine R. Lawrence − *Large-Scale Energy Storage Section, Department of Process and Energy, Faculty of Mechanical Engineering, Delft University of Technology, 2628 CB Delft, The Netherlands; e-Refinery Institute, Delft University of Technology, 2628 CB Delft, The Netherlands*

Complete contact information is available at: https://pubs.acs.org/10.1021/acsenergylett.5c02368

Author Contributions

A.M.I. carried out the experimental work, analyzed the results, and wrote the manuscript. K.R.L. prepared the electrodes, performed SEM measurements, and reviewed the manuscript. R.K. analyzed the results, reviewed the manuscript, and supervised the work.

Notes

The authors declare no competing financial interest.

■ ACKNOWLEDGMENTS

This project has received funding under the NWO-AES Crossover program from project number 17621 (RELEASE). The authors acknowledge Ruud Hendrikx for the X-ray diffraction analysis and Michel van den Brink for lab management and organizing the work environment.

■ REFERENCES

(1) Ma, D.; Jin, T.; Xie, K.; Huang, H. An Overview of Flow Cell Architecture Design and Optimization for Electrochemical CO_2 Reduction. *J. Mater. Chem. A* **2021**, *9* (37), 20897−20918.

(2) Gao, G.; Obasanjo, C. A.; Crane, J.; Dinh, C. T. Comparative Analysis of Electrolyzers for Electrochemical Carbon Dioxide Conversion. *Catal. Today* **2023**, *423*, No. 114284.

(3) Endrődi, B.; Kecsenovity, E.; Samu, A.; Darvas, F.; Jones, R. V.; Török, V.; Danyi, A.; Janáky, C. Multilayer Electrolyzer Stack Converts Carbon Dioxide to Gas Products at High Pressure with High Efficiency. *ACS Energy Lett.* **2019**, *4* (7), 1770−1777.
(4) Burdyny, T.; Smith, W. A. CO_2 Reduction on Gas-Diffusion Electrodes and Why Catalytic Performance Must Be Assessed at Commercially-Relevant Conditions. *Energy Environ. Sci.* **2019**, *12* (5), 1442−1453.
(5) Li, Y. C.; Yan, Z.; Hitt, J.; Wycisk, R.; Pintauro, P. N.; Mallouk, T. E. Bipolar Membranes Inhibit Product Crossover in CO_2 Electrolysis Cells. *Adv. Sustain. Syst.* **2018**, *2* (4), 1−5.
(6) Larrazábal, G. O.; Strøm-Hansen, P.; Heli, J. P.; Zeiter, K.; Therkildsen, K. T.; Chorkendorff, I.; Seger, B. Analysis of Mass Flows and Membrane Cross-over in CO_2 Reduction at High Current Densities in an MEA-Type Electrolyzer. *ACS Appl. Mater. Interfaces* **2019**, *11* (44), 41281−41288.
(7) O'Brien, C. P.; Miao, R. K.; Liu, S.; Xu, Y.; Lee, G.; Robb, A.; Huang, J. E.; Xie, K.; Bertens, K.; Gabardo, C. M.; Edwards, J. P.; Dinh, C.-T.; Sargent, E. H.; Sinton, D. Single Pass CO_2 Conversion Exceeding 85% in the Electrosynthesis of Multicarbon Products via Local CO 2 Regeneration. *ACS Energy Lett.* **2021**, *6* (8), 2952−2959.
(8) Wheeler, D. G.; Mowbray, B. A. W.; Reyes, A.; Habibzadeh, F.; He, J.; Berlinguette, C. P. Quantification of Water Transport in a CO_2 Electrolyzer. *Energy Environ. Sci.* **2020**, *13* (12), 5126−5134.
(9) Endrődi, B.; Samu, A.; Kecsenovity, E.; Halmágyi, T.; Sebők, D.; Janáky, C. Operando Cathode Activation with Alkali Metal Cations for High Current Density Operation of Water-Fed Zero-Gap Carbon Dioxide Electrolysers. *Nat. Energy* **2021**, *6* (4), 439−448.
(10) Gabardo, C. M.; O'Brien, C. P.; Edwards, J. P.; McCallum, C.; Xu, Y.; Dinh, C.-T.; Li, J.; Sargent, E. H.; Sinton, D. Continuous Carbon Dioxide Electroreduction to Concentrated Multi-Carbon Products Using a Membrane Electrode Assembly. *Joule* **2019**, *3* (11), 2777−2791.
(11) Xia, C.; Zhu, P.; Jiang, Q.; Pan, Y.; Liang, W.; Stavitski, E.; Alshareef, H. N.; Wang, H. Continuous Production of Pure Liquid Fuel Solutions via Electrocatalytic CO_2 Reduction Using Solid-Electrolyte Devices. *Nat. Energy* **2019**, *4* (9), 776−785.
(12) Vass, Á.; Kormányos, A.; Kószo, Z.; Endrődi, B.; Janáky, C. Anode Catalysts in CO2 Electrolysis: Challenges and Untapped Opportunities. *ACS Catal.* **2022**, *12*, 1037−1051.
(13) Krause, R.; Reinisch, D.; Reller, C.; Eckert, H.; Hartmann, D.; Taroata, D.; Wiesner-Fleischer, K.; Bulan, A.; Lueken, A.; Schmid, G. Industrial Application Aspects of the Electrochemical Reduction of CO_2 to CO in Aqueous Electrolyte. *Chemie Ing. Technol.* **2020**, *92* (1−2), 53−61.
(14) Xie, K.; Miao, R. K.; Ozden, A.; Liu, S.; Chen, Z.; Dinh, C. T.; Huang, J. E.; Xu, Q.; Gabardo, C. M.; Lee, G.; Edwards, J. P.; O'Brien, C. P.; Boettcher, S. W.; Sinton, D.; Sargent, E. H. Bipolar Membrane Electrolyzers Enable High Single-Pass CO_2 Electroreduction to Multicarbon Products. *Nat. Commun.* **2022**, *13* (1), 3609.

https://doi.org/10.1021/acsenergylett.5c02368
ACS Energy Lett. 2025, 10, 5228−5231